Astron. Astrophys. 340, 497–507 (1998)

ASTRONOMY AND ASTROPHYSICS

Dynamic model atmospheres of AGB stars

I. Atmospheric structure and dynamics

S. Höfner[1,2], U.G. Jørgensen[1], R. Loidl[2], and B. Aringer[2]

[1] Niels Bohr Institute, Astronomical Observatory, Juliane Maries Vej 30, DK-2100 Copenhagen, Denmark
[2] Institut für Astronomie der Universität Wien, Türkenschanzstrasse 17, A-1180 Wien, Austria

Received 16 April 1998 / Accepted 27 August 1998

Abstract. The strong interactions of shock waves caused by stellar pulsation, the formation of molecules and dust grains and a variable radiation field present a considerable challenge when modelling the atmospheres and circumstellar envelopes of pulsating asymptotic giant branch stars. In this paper we present dynamic model atmospheres of long-period variables which allow a consistent computation of near-infrared molecular features and their variability with phase. We discuss the effects of grey radiative transfer, of molecular opacities and of shock waves on the atmospheric structures and on the resulting wind properties. We find that the gas absorption coefficient used in the dynamical calculation has a considerable influence on the structure of the atmosphere, the mass loss and the observable spectral features. Therefore, we stress the importance of using reasonable mean gas opacities in grey dynamic models. Most topics discussed in this paper concern both C- and O-rich atmospheres but the quantitative results are mainly based on C-rich models. Synthetic spectra resulting from selected C- and O-rich models have been presented and compared to observations in several recent papers. A systematic investigation of observable properties of our C-rich models will be the subject of a second paper in this series.

Key words: radiative transfer – hydrodynamics – stars: atmospheres – stars: variables: general – stars: mass-loss – stars: AGB and post-AGB

1. Introduction

The atmospheres of pulsating asymptotic giant branch (AGB) stars are characterized by complicated interactions of time-dependent hydrodynamical processes like shock waves and stellar winds, the formation of molecules and dust grains and a strongly variable stellar radiation field. This presents a severe challenge to constructing appropriate theoretical models and makes the detailed interpretation of observational results difficult (see Bessel & Scholz 1989). Due to the high requirements regarding the numerical treatment of the relevant physics, no self-consistent models exist today that take all of these interacting processes into account simultaneously at a satisfactory level of realism. Two separate approaches, specialising in different aspects of the problem, have been developed: classic hydrostatic model atmospheres and time-dependent dynamic models.

Hydrostatic model atmospheres (reviewed by Gustafsson & Jørgensen 1994) include sophisticated micro-physics (chemistry, etc.) and detailed frequency-dependent radiative transfer both of which are in principle only limited by the available physical input data. With modern computers the radiative transfer problem in standard hydrostatic atmosphere computations can easily be solved for several thousand frequencies during the model iteration process. Several techniques have been developed to handle the line blanketing by molecules in cool stellar atmospheres and impressive results have been obtained for non- or weakly pulsating giants.

Hydrostatic models, however, neglect all dynamical phenomena and thus some fundamental properties of AGB stars like shock waves caused by pulsation and stellar winds. Both have a dramatic influence on the atmospheric structure and the emergent spectrum. During the last few years, instrumental developments like ISO, ground-based IR spectrographs or high-angular-resolution interferometers have lead to an impressive qualitative and quantitative increase of observational data on AGB stars. This again has made the shortcomings of standard hydrostatic model atmospheres more apparent (e.g. Tsuji et al. 1997, Aringer et al. 1997a, 1998).

On the other hand, during the last decade considerable progress has been achieved in using time-dependent dynamical models to predict observational properties of long-period variables. The pioneering work of Bessell et al. (1989, 1996) shows that their models for pulsating M-type Mira variables reproduce observed IR spectra, their temporal variation and the phase and wavelength dependence of photospheric radii reasonably well. Both, these papers and Beach et al. (1988) address the effects of pulsation-extended atmospheres on apparent stellar diameters and the effective temperature scale which is an important issue for determining the mode of pulsation of such stars.

Most dynamical models for C-rich long-period variable atmospheres available in the literature (e.g. Fleischer et al. 1992, Höfner & Dorfi 1997) have been primarily calculated to study dust formation, the role of grains in driving a stellar wind, the structure of the circumstellar envelope as well as the depen-

Send offprint requests to: S. Höfner (hoefner@astro.univie.ac.at)

dence of mass loss on fundamental stellar parameters. These investigations have mainly concentrated on objects with high mass loss rates and more or less optically thick dust envelopes. Typical examples for the predictions of observable properties resulting from such models can be found in the papers of Windsteig et al. (1997) on a comparison of synthetic and observed mid- and far-IR properties (IRAS colours) and of Winters et al. (1997) on a self-consistent model explaining different kinds of observational results for the extreme carbon star AFGL 3068.

Recently, the wide wavelength coverage provided by ISO-SWS has offered the possibility to study simultaneously molecular and dust features and their variability with pulsation phase. This is of particular interest for the investigation of dust-forming objects which are not completely enshrouded in their circumstellar dust shells. Synthetic near-infrared spectra and the variation of molecular features resulting from a low-mass-loss model presented in this paper are in good qualitative agreement with ISO SWS observations of the C-rich AGB star R Scl as shown by Hron et al. (1998).

In summary, the theoretical results for both M- and C-type objects reported in the literature are promising and demonstrate the potential of analysing observational data of pulsating AGB stars with dynamical model atmospheres. Nevertheless, the models are still far from being a solid basis for a detailed quantitative interpretation of observations due to various theoretical approximations and due to restrictions imposed by present-day computing capacities.

One major drawback of time-dependent dynamical models seems to be that they are still restricted to grey radiative transfer. While it should be possible to include frequency-dependent radiative transfer with a very limited number of frequencies in the near future, a full-scale treatment of the problem with thousands of frequencies as in hydrostatic models is far beyond the capacities of present computers. Helling & Jørgensen (1998) investigated in detail the errors introduced in hydrostatic model atmospheres by picking a successively smaller number of frequency points in the opacity sampling, and compared the resulting structures with models based on simple mean opacities. However it remains to be demonstrated that non-grey radiative transfer in dynamical models with such a small number of frequency points as can be handled in this context is actually an improvement compared to grey models based on reasonable mean opacities.

In the present paper, we study the influence of the gas opacity (molecules) and of time-dependent dynamics on the structure of the model atmospheres and on the resulting wind properties (Sects. 3 and 4, respectively). To estimate the uncertainties introduced by using grey radiative transfer in the dynamical calculations we compare the hydrostatic limit case of our grey models to classical hydrostatic model atmospheres with full non-grey radiative transfer using the corresponding frequency-dependent molecular opacities. A major point is to demonstrate that the use of Planck mean opacities based on molecular data gives much more realistic atmospheric structures than a constant gas absorption coefficient used in many earlier dynamic calculations (Sect. 2).

Although we are aware that the Planck mean is not the theoretically correct, and therefore by no means final absorption coefficient to apply in the atmospheric radiative transfer, we emphasize that the presented grey dynamic models permit us to study dynamical phenomena and their effects on observable properties in a self-consistent way. The improved models presented here allow us to produce reasonable synthetic spectra by adjusting nothing else but the fundamental stellar parameters and the pulsation characteristics.

Synthetic spectra resulting from selected models are discussed and compared to observations by Loidl et al. (1997, 1998), Höfner et al. (1998), Hron et al. (1997, 1998) and Aringer et al. (1997b, 1998). A systematic analysis of observable properties of our C-rich models will be presented by Loidl et al. in a second paper in this series.

2. Modelling method and parameters

We obtain the variable spatial structure of the atmosphere and circumstellar envelope (density, temperature, degree of condensation, etc.) by solving the equations of grey radiation hydrodynamics together with a time-dependent description of the dust formation (see Höfner & Dorfi 1997, Höfner et al. 1995 and references therein for details of the modelling method). The gas dynamics (including self-gravity) is described by the equations of continuity, motion and energy. The radiation field is determined by the grey moment equations of the radiative transfer equation, closed by a variable Eddington factor. The energy exchange between matter and radiation adopts a LTE source function which results in extremely (possibly too) efficient cooling behind radiative shocks (for a detailed discussion of cooling rates we refer to Willson & Bowen 1998 and Woitke et al. 1996).

The dynamic calculations start with an initial model which represents the full hydrostatic limit case of the grey radiation hydrodynamics equations, including a variable Eddington factor. It is determined by the following parameters: luminosity $L_\star$, mass $M_\star$, effective temperature $T_\star$ and the elemental abundances. In the calculations presented here all elemental abundances are assumed to be solar except the one of carbon which is specified by an additional parameter, i.e. the carbon-to-oxygen ratio $\varepsilon_{\rm C}/\varepsilon_{\rm O}$. The structure of this hydrostatic initial model can be directly compared to standard model atmospheres (see Sect. 3.1).

The stellar pulsation is simulated by a variable boundary (piston) located beneath the stellar photosphere and moving with a velocity amplitude $\Delta u_{\rm p}$ and a period P. Since this boundary condition (and especially the parameter $\Delta u_{\rm p}$) has a considerable influence on the global atmospheric structure and the stellar wind (Sect. 3.2 and 4) an important future goal is to replace it with a more consistent one resulting from pulsational models. A further step to be taken is the construction of models which contain the pulsation zone as well as the atmosphere and stellar wind region. An alternative to the assumption of a simple piston boundary condition was introduced by Bessell et al. (1996) who based their photospheric models on the dynamic models of Wood (1990). These models include the driving zone of the pulsation but introduce a depth-dependent free parameter (artificial

Table 1. Model parameters ($L_\star$, $M_\star$, $T_\star$, $\varepsilon_{\rm C}/\varepsilon_{\rm O}$, P, $\Delta u_{\rm p}$) and results: mass loss rate $\dot{M}$, mean velocity at the outer boundary $\langle u\rangle$, mean degree of condensation at the outer boundary $\langle f_{\rm c}\rangle$; $\kappa_{\rm g}$ is the gas absorption coefficient used for the model (mol-P: Planck mean, based on the SCAN molecular line data; see text). $R_\star$ is the stellar radius of the hydrostatic initial model (calculated from $L_\star$ and $T_\star$) and, for convenience, we also list the corresponding $\lg g_\star$. The dust-to-gas ratio ρ_d/ρ_g is calculated from $f_{\rm c}$ as described in HD97 involving $\varepsilon_{\rm C}/\varepsilon_{\rm O}$ as the only model-dependent quantity. Outflow velocities listed in brackets indicate models where $\langle u\rangle$ is below the local escape velocity. The corresponding mass loss rates should be considered as uncertain. 'T' indicates a transition model (see text) and '-' means that the model does not show mass loss by a stellar wind.

model	$\kappa_{\rm g}$ [cm^2/g]	$L_\star$ [$L_\odot$]	$M_\star$ [$M_\odot$]	$T_\star$ [K]	$R_\star$ [$R_\odot$]	$\lg g_\star$	C/O	P [d]	$\Delta u_{\rm p}$ [km/s]	$\dot{M}$ [M$_\odot$/yr]	$\langle u\rangle$ [km/s]	$\langle f_{\rm c}\rangle$	ρ_d/ρ_g [10^{-3}]
P7C12U4	mol-P	7000	1.0	2880	336	−0.61	1.20	390	4.0	–	–	–	–
P7C14U2	mol-P	7000	1.0	2880	336	−0.61	1.40	390	2.0	–	–	–	–
P7C14U4	mol-P	7000	1.0	2880	336	−0.61	1.40	390	4.0	T	T	(0.3)	(0.7)
P7C14U6	mol-P	7000	1.0	2880	336	−0.61	1.40	390	6.0	$2.6\cdot10^{-7}$	(2)	0.36	0.8
P7C18U4	mol-P	7000	1.0	2880	336	−0.61	1.80	390	4.0	$2.2\cdot10^{-7}$	7	0.13	0.6
P10C14U4	mol-P	10000	1.0	2790	428	−0.82	1.40	525	4.0	$6.6\cdot10^{-7}$	(3)	0.19	0.4
P10C18U2	mol-P	10000	1.0	2790	428	−0.82	1.80	525	2.0	$1.9\cdot10^{-7}$	9	0.05	0.2
P10C18U4	mol-P	10000	1.0	2790	428	−0.82	1.80	525	4.0	$1.0\cdot10^{-6}$	14	0.14	0.6
P10C18U6	mol-P	10000	1.0	2790	428	−0.82	1.80	525	6.0	$2.3\cdot10^{-6}$	17	0.23	1.0
P13C12U4	mol-P	13000	1.0	2700	521	−0.99	1.20	650	4.0	$5.7\cdot10^{-7}$	(2)	0.33	0.4
P13C14U4	mol-P	13000	1.0	2700	521	−0.99	1.40	650	4.0	$2.9\cdot10^{-6}$	11	0.25	0.6
P13C14U6	mol-P	13000	1.0	2700	521	−0.99	1.40	650	6.0	$5.5\cdot10^{-6}$	12	0.28	0.6
P7TC14U4	mol-P	7000	1.0	2970	316	−0.56	1.40	390	4.0	–	–	–	–
P10TC14U4	mol-P	10000	1.0	2880	401	−0.77	1.40	525	4.0	$5.7\cdot10^{-7}$	(3)	0.19	0.4
P10MC14U4	mol-P	10000	1.4	2790	428	−0.67	1.40	525	4.0	T	T	(0.3)	(0.7)
P5OU2[a]	mol-P	5000	1.0	2970	267	−0.41	0.48	295	2.0	$4\cdot10^{-9}$	(3)	no dust	
P5tOU2[a]	mol-P	5000	1.0	2880	287	−0.48	0.48	295	2.0	$9\cdot10^{-9}$	(3)	no dust	
P5tOU3[a]	mol-P	5000	1.0	2880	287	−0.48	0.48	295	3.0	$9\cdot10^{-9}$	(3)	no dust	
P5tOU4[a]	mol-P	5000	1.0	2880	287	−0.48	0.48	295	4.0	$2\cdot10^{-8}$	(4)	no dust	
P7OU2	mol-P	7000	1.0	2880	336	−0.61	0.48	390	2.0	$9.6\cdot10^{-8}$	12	no dust	
P7OU4	mol-P	7000	1.0	2880	336	−0.61	0.48	390	4.0	$1.2\cdot10^{-6}$	12	no dust	
P7OU6	mol-P	7000	1.0	2880	336	−0.61	0.48	390	6.0	$2.1\cdot10^{-6}$	12	no dust	
K7U4[b]	$1\cdot10^{-2}$	7000	1.0	2880	336	−0.61	1.80	390	4.0	$5.8\cdot10^{-7}$	13	0.44	2.0
R7C18[c]	$2\cdot10^{-4}$	7000	1.0	2880	336	−0.61	1.80	390	2.0	$5.8\cdot10^{-7}$	7	0.37	1.7
R10C18[c]	$2\cdot10^{-4}$	10000	1.0	2790	428	−0.82	1.80	525	2.0	$1.6\cdot10^{-5}$	25	0.71	3.2
R13[c]	$2\cdot10^{-4}$	13000	1.0	2700	521	−0.99	1.40	650	2.0	$5.9\cdot10^{-6}$	7	0.45	1.0
R13U[c]	$2\cdot10^{-4}$	13000	1.0	2700	521	−0.99	1.40	650	6.0	$4.5\cdot10^{-5}$	13	0.60	1.4

[a] used by Aringer et al. (1998) [b] used by Loidl et al. (1997), Alvarez & Plez (1998) [c] from Höfner & Dorfi (1997)

damping/growth factor) into the energy conservation equation which is adjusted by trial and error to produce the desired non-linear pulsation amplitude. To avoid the physical and technical problems involved in such a treatment of the pulsation we have adopted the simple approach of a moving piston at the inner boundary of the model which should be a reasonable first-order approximation of the dynamical effects of stellar pulsation on the atmosphere. This assumption enables us to focus our attention on improving the description of the stellar atmosphere and makes the comparison with other models and previous work easier.

The models presented here have been improved compared to those in Höfner & Dorfi (1997; HD97) by a more realistic treatment of the gas opacity. In HD97 a constant value (i.e. independent of thermodynamical conditions and of chemical composition) has been used for the gas absorption coefficient as introduced in the pioneering work of Bowen (1988; for O-rich Mira models) and used by many other time-dependent calculations in the literature (e.g. Fleischer et al. 1992). The constant value of $\kappa_{\rm g} = 2\cdot10^{-4}{\rm cm}^2/{\rm g}$ was chosen by Bowen (1988) on the basis that it leads to the same structure in the surface layers of a given model of an oxygen-rich Mira star as was obtained with a detailedly calculated Rosseland mean $\kappa_{\rm g}$ for the same model. In the present work this constant value is replaced by Planck mean absorption coefficients which are based on the SCAN molecular line data (Jørgensen 1997) and which are computed for the relevant values of temperature, density and chemical composition in the star. While this frequency-independent treatment of radiative transfer is still a crude approximation, the resulting atmospheric structures are in much better agreement with

frequency-dependent model atmospheres than those of HD97 (see Sect. 3.1). We find that the gas opacity used in the dynamical calculation plays a crucial role with regard to the resulting near-IR spectra (Höfner et al. 1998) and wind properties of the models (Sect. 4). A detailed discussion about the effects of using Rosseland mean opacities in dynamical models of M-type stars can be found in Bessell et al. (1996)

In this paper we mainly consider models for C-rich stars which include the formation of amorphous carbon grains. The results concerning mass loss are compared to those of HD97 in Sect. 4 and exemplary synthetic spectra can be found in the papers mentioned in Sect. 1. Several models for O-rich stars without dust formation are included in this paper for comparison with the C-rich models and to discuss the role of molecular opacities in driving stellar winds. Molecular spectra resulting from some of these models have been computed and compared to observations by Aringer et al. (1997b, 1998).

The combinations of the stellar parameters $L_\star$, $M_\star$, $T_\star$ and P are chosen in accordance with HD97 (based on radius-mass-luminosity and period-luminosity relations; see explanations given there) except for a few models where one of these parameters has been changed to show its influence on the model (P7TC14U4, P10TC14U4, P10MC14U4; see Table 1). The remaining parameters $\varepsilon_{\rm C}/\varepsilon_{\rm O}$ and $\Delta u_{\rm p}$ have been varied in the present models to investigate the influence of chemical composition via the gas opacities and to (partially) compensate lower densities in the hydrostatic initial models caused by the new gas opacities (see Sect. 3.1 and 4).

3. Atmospheric structure

The models of HD97 were calculated mainly to investigate the circumstellar dust shell and its temporal variations as well as mass loss and its dependence on various model parameters. When calculating the first experimental synthetic spectra based on these models, we found that the computed molecular features were far too strong compared to observed ones. This is due to the fact that the models have a too high overall density since the constant gas absorption coefficient used there (see Sect. 2) tends to underestimate the gas opacity in most layers of the stellar atmosphere. Therefore we have improved our dynamic models by using a more realistic gas absorption coefficient.

In this section we discuss the influence of gas opacity and of time-dependent dynamics (i.e. shock waves and wind) on the stellar atmosphere and compare our grey initial models to standard hydrostatic model atmospheres. Stellar wind properties like mass loss rates and dust formation are discussed in Sect. 4.

3.1. The hydrostatic limit case

In the dust-free hydrostatic limit the structure of our grey models can be directly compared to standard hydrostatic model atmospheres based on frequency-dependent radiative transfer. The latter are calculated using the MARCS code (Gustafsson et al. 1975) in the version of Jørgensen et al. (1992). The radiative transfer is computed in about 5000 frequencies where the molecular absorption coefficients are treated by use of the opacity sampling method.

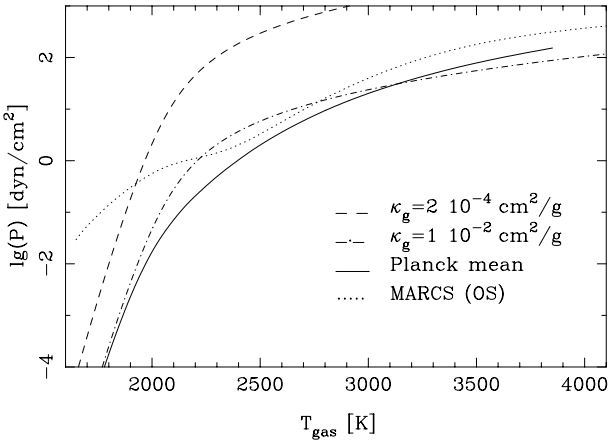

Fig. 1. Atmospheric structure (gas pressure vs. temperature) of hydrostatic models: the grey initial model P7C14 (full line; based on Planck mean molecular absorption coefficients) and two models calculated with the same stellar parameters but constant gas opacity (dashed: R7C18, $\kappa_{\rm g} = 2 \cdot 10^{-4}$ cm^2/g; dash-dotted: K7U4, $\kappa_{\rm g} = 10^{-2}$ cm^2/g) as well as a MARCS model atmosphere with similar stellar parameters (dotted; based on full monochromatic opacity sampling of the same molecular data as in model P7C14).

In Fig. 1 we show the pressure-temperature structure of several grey hydrostatic initial models, i.e. R7C18 (dashed), K7U4 (dash-dotted) and P7C14[1] (full line), in comparison to a MARCS model atmosphere (dotted). All models in Fig. 1 have the same stellar parameters, i.e. $L_\star = 7000\,L_\odot$, $M_\star = 1\,M_\odot$ and $T_\star = 2880$ K. For models with $\kappa_{\rm g} = $ const (R7C18 and K7U4 in Fig. 1) $\varepsilon_{\rm C}/\varepsilon_{\rm O}$ only enters via dust formation and is thus irrelevant for the comparison of the dust-free initial models. The other models shown in Fig. 1 have $\varepsilon_{\rm C}/\varepsilon_{\rm O}$=1.4. The main difference between the various models is the treatment of radiative transfer: grey approximation with different gas absorption coefficients $\kappa_{\rm g}$ and full monochromatic opacity sampling (MARCS).

The MARCS model atmosphere (dotted) is considered as the 'ideal model' in Fig. 1 because it contains the most detailed radiative transfer.

The dashed line corresponds to model R7C18 of HD97. Due to the low value of $\kappa_{\rm g} = 2 \cdot 10^{-4}{\rm cm}^2/{\rm g}$ (Bowen 1988; see Sect. 2) this model has a much higher overall gas pressure than the MARCS atmosphere. In model K7U4 (dash-dotted) the constant value of $\kappa_{\rm g}$ has been increased to $10^{-2}{\rm cm}^2/{\rm g}$ to reach roughly the same overall density as in the MARCS model. While this leads to relatively reasonable synthetic spectra (Loidl et al. 1997; Alvarez & Plez 1998), at least compared to R7C18,

[1] The names of the new dynamical models (series P) contain a U followed by a number which represents the piston velocity amplitude $\Delta u_{\rm p}$ in km/s. The corresponding hydrostatic initial models are denoted by the same name without the U and subsequent number because $\Delta u_{\rm p}$ does not apply there.

this choice of $\kappa_{\rm g}$ is rather arbitrary and the atmospheric structure is still far from resembling the MARCS model.

The full line represents the initial model P7C14. It is calculated using Planck mean opacities based on the same molecular opacity data (SCAN, Jørgensen 1997) as used in the MARCS model (dotted), yielding a reasonably realistic atmospheric structure which is largely comparable to the MARCS model, except in the outermost parts of the model. The discrepancy in the optically thin upper layers is obviously due to non-grey effects since all grey models show a steep decline of the pressure whereas the MARCS atmospheres generally have a much smaller pressure gradient there. The importance of this difference is, however, limited by the fact that these atmospheric layers are severely affected by dynamical effects[2] (levitation, passing shocks) as will be demonstated in Sect. 3.2.

A comparison of the structures of models K7U4 ($\kappa_{\rm g}$ = const; dash-dotted) and P7C14 (Planck mean; full line) might suggest that little has been gained by substituting the constant gas absorption coefficient with a (technically more complicated) Planck mean. A closer inspection, however, reveals some fundamental differences. First, the rough agreement between the MARCS model and K7U4 is only achieved by adjusting the value of $\kappa_{\rm g}$ in such a way that the partial pressures and thus the resulting spectra are somehow reasonable. This is done to demonstrate the influence of $\kappa_{\rm g}$ in a simple way, but one has to keep in mind that this quantity is not a free parameter. Using a Planck mean instead eliminates this unphysical extra parameter. Secondly, without any possibility of fitting, the Planck mean leads to a structure of the atmosphere that is in relative good agreement with a frequency-dependent model based on the same opacity input-data. The pressure-temperature structure of model P7C14 qualitatively resembles the MARCS model, running parallel in the lower atmospheric layers, whereas model K7U4 shows a different pressure gradient. In the outermost layers both grey models differ a lot from the MARCS atmosphere, but this is most likely a general problem of the grey radiative transfer as mentioned before.

Even the seemingly small differences in the structures of K7U4 and P7C14 lead to remarkable effects in the resulting synthetic spectra and colours. These limitations should be kept in mind when interpreting results based on models with constant $\kappa_{\rm g}$ (e.g. Loidl et al. 1997, Alvarez & Plez 1998). A comparison of synthetic spectra resulting from models K7U4 and P7C14U4 can be found in Höfner et al. (1998).

A qualitatively new feature compared to HD97 is the dependence of $\kappa_{\rm g}$ on $\varepsilon_{\rm C}/\varepsilon_{\rm O}$. Consequently, even the dust-free parts of the models are affected by the chemical composition now, whereas in the former models $\varepsilon_{\rm C}/\varepsilon_{\rm O}$ only entered via the dust component and its indirect influence on the structure. In Fig. 2 we show the effects of different $\varepsilon_{\rm C}/\varepsilon_{\rm O}$ values on hydrostatic inital models (P7C12: $\varepsilon_{\rm C}/\varepsilon_{\rm O} = 1.2$, dashed; P7C14: $\varepsilon_{\rm C}/\varepsilon_{\rm O} = 1.4$, full; P7C18: $\varepsilon_{\rm C}/\varepsilon_{\rm O} = 1.8$, dash-dotted; P7O: $\varepsilon_{\rm C}/\varepsilon_{\rm O} = 0.48$, dotted) where all other parameters are the same. The influence on the dust formation and stellar wind will be discussed in Sect. 4.

[2] Furthermore, it is unclear to which extent Doppler shifts caused by the velocity field might influence the integrated absorption coefficients which are relevant for the energy and momentum balance and thus for the structure of the atmosphere. This could actually make Planck means which rather tend to over-estimate the opacity in a hydrostatic structure a reasonable choice in dynamical models.

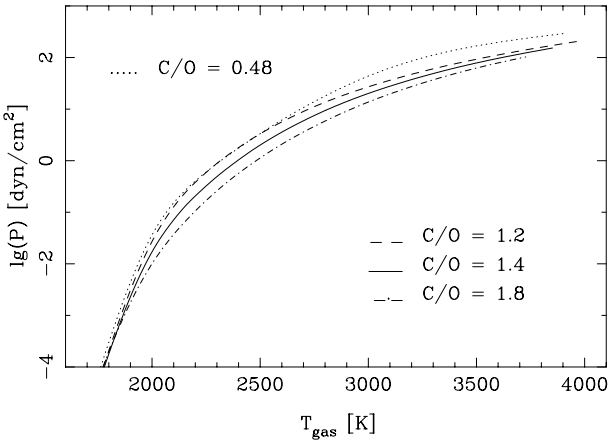

Fig. 2. Atmospheric structure (gas pressure vs. temperature) of hydrostatic initial models: influence of the carbon-to-oxygen ratio; P7C12 ($\varepsilon_{\rm C}/\varepsilon_{\rm O} = 1.2$, dashed), P7C14 ($\varepsilon_{\rm C}/\varepsilon_{\rm O} = 1.4$, full line), P7C18 ($\varepsilon_{\rm C}/\varepsilon_{\rm O} = 1.8$, dash-dotted) and P7O ($\varepsilon_{\rm C}/\varepsilon_{\rm O} = 0.48$, dotted).

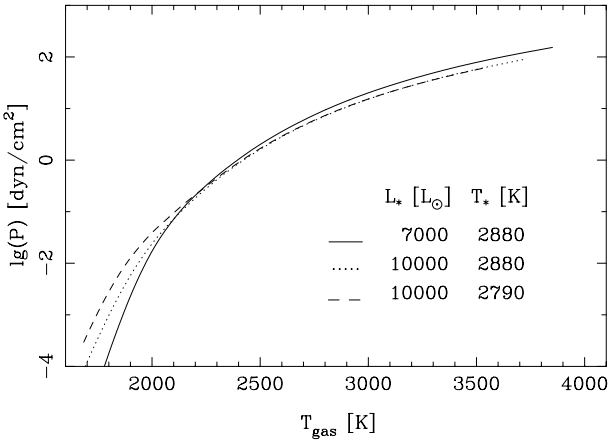

Fig. 3. Atmospheric structure (gas pressure vs. temperature) of hydrostatic initial models: influence of stellar parameters $L_\star$ and $T_\star$; P7C14 (full), P10C14 (dashed), P10TC14 (dotted).

Fig. 3 demonstrates the influence of $L_\star$ and $T_\star$ on the pressure-temperature structure while all other parameters are kept constant. Models P10C14 (dashed) and P10TC14 (dotted) differ by $T_\star$ only. Their structures are quite similar below the photosphere but further out the hotter model P10TC14 exhibits a lower gas pressure at a given temperature. P10TC14 (dotted) and P7C14 (full line) have identical parameters except $L_\star$. The less luminous model P7C14 shows a steeper slope throughout the atmosphere but the differences are more pronounced in the outer zones of the models. The combined influence of $L_\star$ and $T_\star$ on the atmospheric structure is demonstrated by a comparison of P7C14 (full) and P10C14 (dashed). Note, how the atmosphere becomes more extended (smaller pressure gradient) with

increasing $L_\star$ and decreasing $T_\star$. Model P10MC14 (not shown in Fig. 3) allows one to study the influence of $M_\star$. Except for a higher mass, its parameters are identical to P10C14 (dashed) but its pressure-temperature structure is almost identical with model P7C14 (full line).

In conclusion from Figs. 1–3, the difference in the hydrostatic model structures which results from the various gas absorption coefficients we have tested is much larger than the differences resulting from (1) varying $\varepsilon_{\rm C}/\varepsilon_{\rm O}$ between 1.2 and 1.8 (corresponding to most of the bright carbon stars seen in the sky), (2) varying $L_\star/L_\odot$ between 7000 and 10000, (3) varying $T_\star$ between 2790 K and 2880 K, or (4) varying $M_\star/M_\odot$ between 1 and 1.4. The difference between the two models based on the same molecular data but sampled in two different ways (Planck mean and opacity sampling treatment, respectively) is largest in the upper atmospheric layers where the opacity sampling model has some orders of magnitude higher gas pressure than the Planck model, as seen in Fig. 1. The difference between the Planck models and the models based on the constant $\kappa_{\rm g}$ used previously in hydrodynamic calculations in the literature is huge throughout the model, amounting to about two orders of magnitude in the gas pressure at a given temperature.

For a better comparability with previous work the models shown in Figs. 1–3 are C-rich with the only exception of model P7O in Fig. 2. However, we want to emphasize that qualitatively similar conclusions can be drawn for our O-rich models, in spite of some natural quantitative differences between C- and O-rich models.

After presenting our progress in optimizing the grey radiative transfer we will now discuss the influence of shock waves and stellar winds on the atmospheric structure.

3.2. Effects of time-dependent dynamics

Since most AGB stars are known to be large amplitude pulsators, time-dependent dynamic phenomena which severely affect the atmospheric structure have to be taken into account properly. The stellar pulsation of the long-period variable creates shock waves in the atmosphere which basically influence the structure in two ways (see Fig. 4): In the inner part of the model the passing shocks cause a periodic modulation of the pressure-temperature structure which varies around that of the corresponding hydrostatic initial model. Further out (below $\approx$ 2000 K in Fig. 4) the shocks induce a levitation of the atmosphere, providing at all phases much higher densities than in the hydrostatic model. This favours the formation of molecules and dust grains, and eventually leads to the onset of a dust-driven wind.

As demonstrated by Fig. 4 the levitation depends strongly on the piston velocity amplitude $\Delta u_{\rm p}$ applied at the inner boundary. The two models shown differ only by $\Delta u_{\rm p}$. Model P7C14U2 (upper panel, $\Delta u_{\rm p}$ = 2 km/s) exhibits a much smaller levitation than model P7C14U4 (lower panel, $\Delta u_{\rm p}$ = 4 km/s). Since several pronounced molecular features are formed in this region, $\Delta u_{\rm p}$ has a considerable effect on the resulting synthetic spectra.

The local modulations caused by the running shock waves change the structure of the atmosphere in a way which cannot be simulated by a sequence of hydrostatic atmospheres. First experimental studies (e.g. Aringer et al. 1997b, 1998, Alvarez & Plez 1998) seem to indicate that our dynamic models are able to reproduce observed high-resolution molecular spectra and out-of-phase variation of photometric colours, at least at a qualitative level. Another promising test for the models are line profile variations of CO lines (e.g. Windsteig et al. 1998). A comparison of synthetic IR spectra resulting from model P7C14U4 with ISO-SWS spectra of R Scl is presented by Hron et al. (1998).

Fig. 5 shows the radial structure of the flow velocity (a), the gas density (b), the temperature (c) and the degree of condensation (d) of model P7C14U4 at four different phases of the pulsation cycle as well as the corresponding hydrostatic initial model (full line). The shock fronts created by the pulsation first increase rapidly in strength (up to $\approx$ 20 km/s; Fig. 5a) as they move outwards along the steep density gradient of the in-

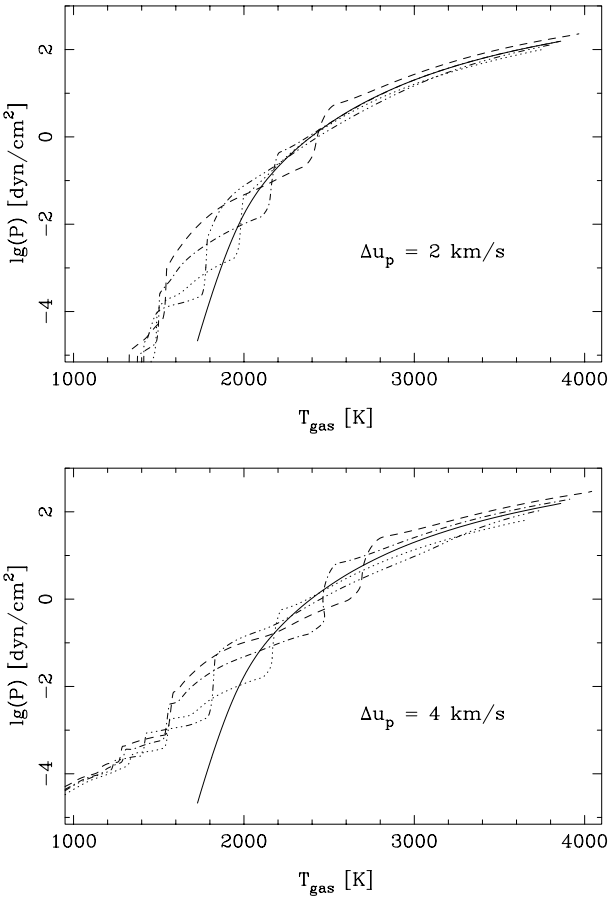

Fig. 4. Atmospheric structure (gas pressure vs. temperature) of models P7C14U2 (*upper panel*) and P7C14U4 (*lower panel*) at different phases (0.50: dashed; 0.75: dash-dotted; 1.00: dotted; 1.25: dash-triple-dot) and of the corresponding hydrostatic initial model (full line); phase 0.5 corresponds to minimum light, 1.0 to maximum light. The 'steps' in the pressure indicate shock waves. Their propagation through the atmosphere can be seen by tracking the progress of individual features from higher pressures and temperatures to lower ones (i.e. from right to left) with increasing time (phase 0.5 to 1.25). Note that the two models differ by $\Delta u_{\rm p}$ only (P7C14U2: 2 km/s; P7C14U4: 4 km/s).

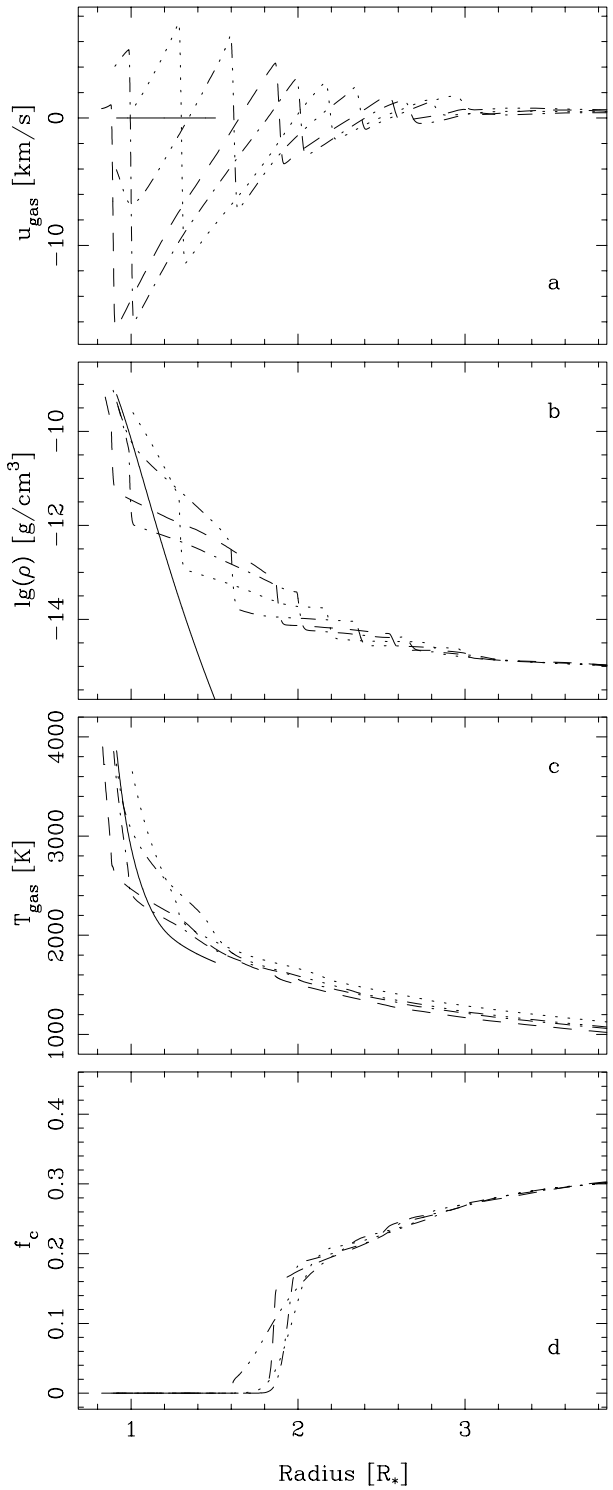

Fig. 5a–d. Radial structure of model P7C14U4 at different phases (0.50: dashed; 0.75: dash-dotted; 1.00: dotted; 1.25: dash-triple-dot) and of the corresponding hydrostatic initial model (full line); flow velocity **a**, gas density **b**, gas temperature **c** and degree of condensation **d** as a function of the radius (given in units of the radius of the hydrostatic initial model).

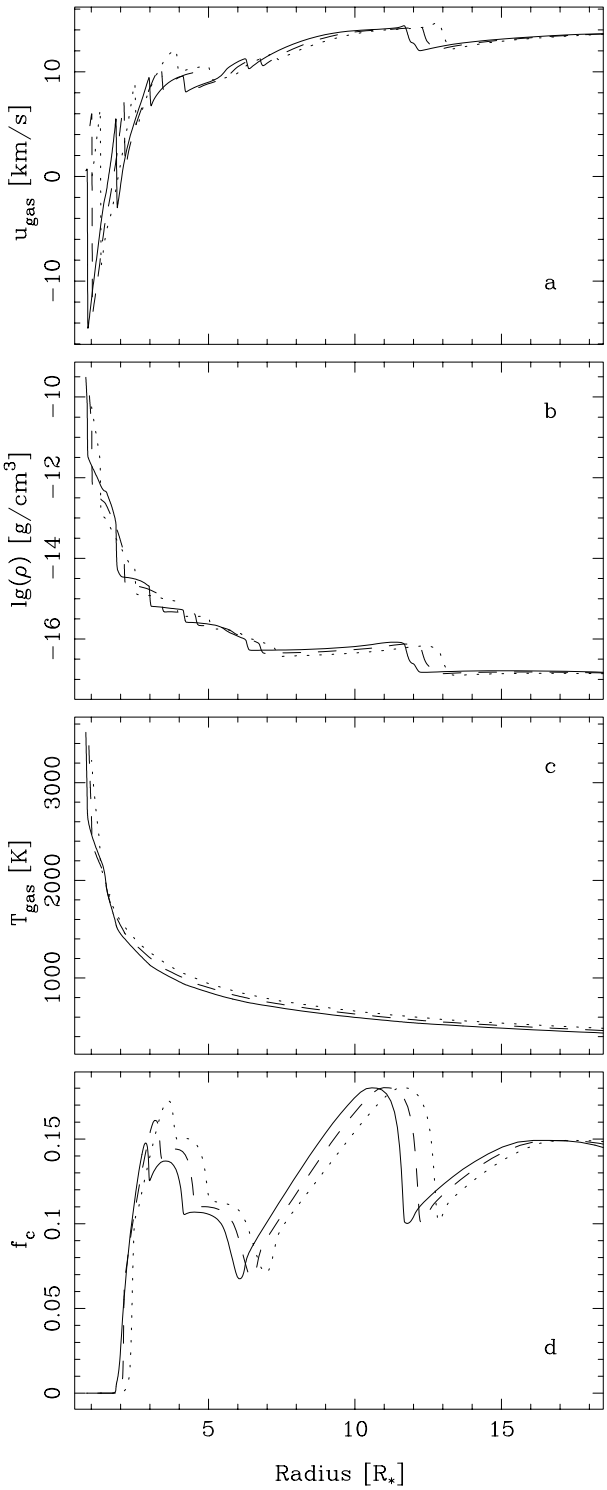

Fig. 6a–d. Radial structure of model P10C18U4 at different phases (time sequence: full, dashed, dotted): flow velocity **a**, gas density **b**, gas temperature **c** and degree of condensation **d** as a function of the radius (given in units of the radius of the hydrostatic initial model).

ner atmosphere. Then they gradually become weaker again as they move further out, against the infalling material in the wake of the preceeding shock wave (positive velocity means outflowing, negative velocity infalling material). The gas is compressed in the shock fronts, leading to the 'steps' in the density struc-

ture (Fig. 5b). As in the pressure-temperature plot (Fig. 4, lower panel) both dynamical effects on the structure are clearly visible here: the modulation by passing shocks in the inner part of the model and the levitation further out. Note the huge density increase at a given radius compared to the hydrostatic model.

Model P7C14U4 is a 'transition model' between a dust-free dynamic atmosphere and a dust-driven stellar wind. Though a certain amount of dust forms in this model it is not sufficient to drive an outflow. The relatively low luminosity just keeps the dust envelope in balance, preventing the infall of material pushed out by shocks on a large scale. For comparison the radial structure of a typical wind model, P10C18U4, is shown in Fig. 6: the flow velocity (a), the gas density (b), the temperature (c) and the degree of condensation (d). The average dust-to-gas ratio of P7C14U4 is about the same (higher degree of condensation but smaller amount of condensible carbon) as for model P10C18U4 where the higher luminosity is sufficient to drive a stellar wind. Note the different radial scales in Figs. 5 and 6.

4. Wind properties

In this section we discuss how the gas opacities influence the wind properties (mass loss rate, outflow velocity, dust properties) of our models. For this purpose, we have calculated a small set of C-rich models with the same parameters as in HD97 with the exception of $\Delta u_{\rm p}$ which was varied to compare its influence on the model with the effects of the dramatic change of the gas density due to the new $\kappa_{\rm g}$. In this sense models P7C18U4, P10C18U2/U4/U6 and P13C14U4/U6 correspond to R7C18, R10C18 and R13/U, respectivly. Note that P10C18U2 and R10C18 as well as P13C14U6 and R13U have identical parameters, including $\Delta u_{\rm p}$.

Fig. 7 (top) shows a comparison of the resulting mass loss rates. The full symbols correspond to the new models and the open symbols to the results of HD97. All models with a given $L_\star$ have the same parameters, except the piston velocity amplitude $\Delta u_{\rm p}$ which is indicated by the shape of the symbol. For identical model parameters (same symbol shape) the mass loss rates of the new models are considerably lower than in HD97, as expected from the lower overall density (see Sect. 3 and Fig. 8). This effect can partly be compensated by increasing the piston velocity amplitude $\Delta u_{\rm p}$, which affects the density in the wind acceleration zone (levitation).

The lines in Fig. 7 represent the values calculated from the mass loss formula of Arndt et al. (1997) for the corresponding parameters (full line: $\varepsilon_{\rm C}/\varepsilon_{\rm O} = 1.8$, $\Delta u_{\rm p} = 2\,$km/s, dashed: $\varepsilon_{\rm C}/\varepsilon_{\rm O} = 1.8$, $\Delta u_{\rm p} = 4\,$km/s, dotted: $\varepsilon_{\rm C}/\varepsilon_{\rm O} = 1.4$, $\Delta u_{\rm p} = 2\,$km/s; $T_\star = T_\star(L_\star)$, $P = P(L_\star)$, $M_\star = 1 M_\odot$; see Table 1). The formula was derived from the models of Fleischer et al. (1992; based on the same constant $\kappa_{\rm g}$ as the models of HD97) and Arndt et al. (1997) found it to be in reasonable agreement with the results of HD97. All of our new models, however, fall distinctly below their predicted values, clearly illustrating the large importance of the adopted gas opacity also on gross dynamical properties as the mass loss rate.

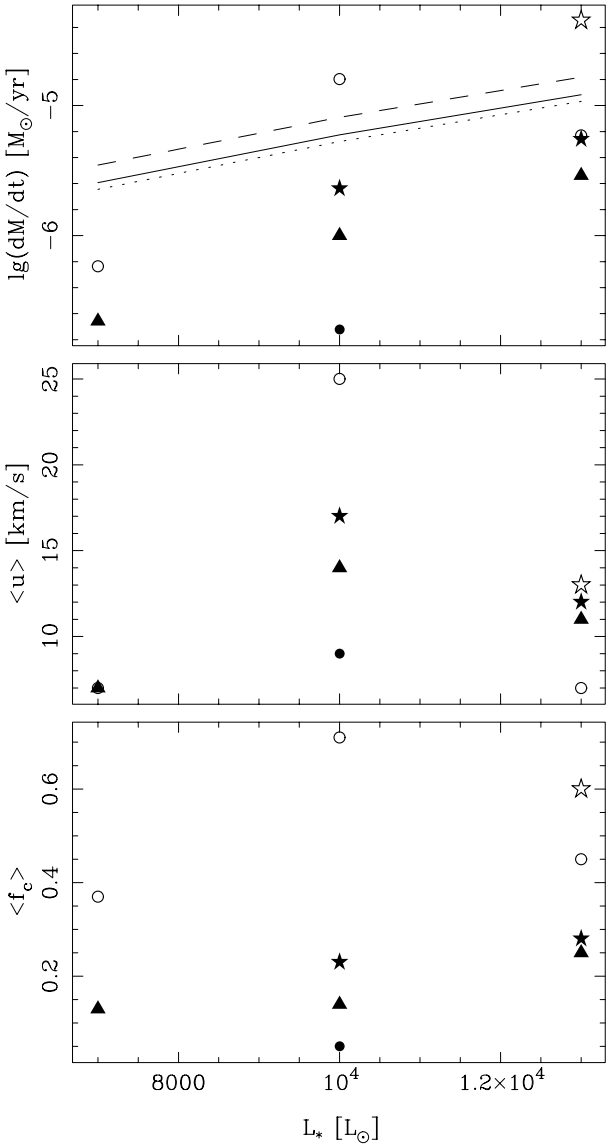

Fig. 7. Comparison of mass loss rates (*top*), outflow velocities (*center*) and degrees of condensation (*bottom*) of C-rich models: selected models of Höfner & Dorfi (1997; R7C18, R10C18, R13, R13U; open symbols) and this work (P7C18, P10C18U2/U4/U6, P13C14U4/U6; full symbols). The shape of the symbol indicates the piston velocity amplitude of the model ($\Delta u_{\rm p}$: ○ = 2 km/s, △ = 4 km/s, ⋆ = 6 km/s), the other stellar parameters are the same for all models with a given $L_\star$ (see text). The lines correspond to values calculated form the mass loss formula of Arndt et al. (1997), for details see text.

Our new models show significantly lower final degrees of condensation (< 0.3, Fig. 7, bottom) than those of HD97, reflecting reduced grain growth rates due to the lower gas density. A second reason why the degree of condensation is relatively low for almost all new models in Table 1 may be the fact that the gas density now also depends on $\varepsilon_{\rm C}/\varepsilon_{\rm O}$ (see Sect. 3). In the models of HD97 an increase of $\varepsilon_{\rm C}/\varepsilon_{\rm O}$ directly resulted in an increase of the partial pressures of those molecules that contribute to the dust formation and grain growth. In the present work, these molecules contribute significantly to the gas absorption coeffi-

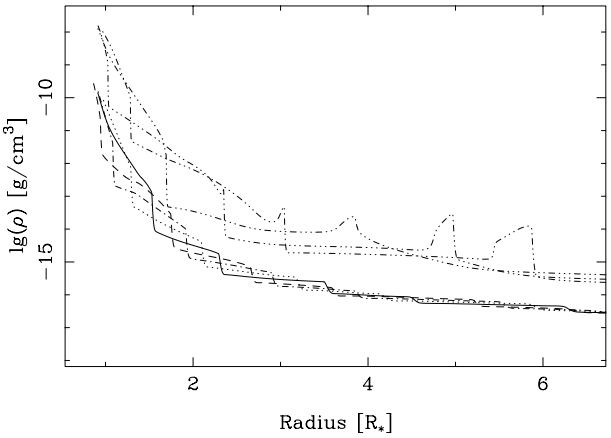

Fig. 8. Density as a function of radius for model P10C18U2 (phases: 0.50: dashed; 0.75: dash-dotted; 1.00: dotted; 1.25: full line) and R10C18 (dash-triple-dot lines, random phases). Due to the low gas absorption coefficient used in model R10C18 the density is 1-2 orders of magnitude higher throughout the model.

cient and therefore a certain self-regulating mechanism exists: The higher abundance of the molecules causes a higher opacity and consequently a higher radiation pressure which again leads to a decrease of the gas pressure. This effect is demonstrated by Fig. 2 which shows inital models that differ by $\varepsilon_{\rm C}/\varepsilon_{\rm O}$ only.

Therefore, the simple rule that higher $\varepsilon_{\rm C}/\varepsilon_{\rm O}$ means a higher degree of condensation, seems to break down for models that take the molecular opacities self-consistently into account. This again could lead to a qualitatively different dependence of the wind properties on $\varepsilon_{\rm C}/\varepsilon_{\rm O}$ than described in Arndt et al. (1997).

The wind velocities (Fig. 7, center) are approximately the same as before, or at least not reduced by the same amount as the degree of condensation. This seems to indicate that in our present models radiation pressure on molecules contributes to driving the stellar winds, since the outflow velocity of a dust driven wind should be closely correlated to the dust opacity and therefore to the degree of condensation (see HD97 for details).

The O-rich models listed in Table 1 (P5OU2, P5tOU2/U3/U4, P7OU2/U4/U6; all calculated without dust formation) seem to support this conclusion. While the models with $L_\star = 5000\,L_\odot$ only show a negligible mass loss an increase to $7000\,L_\odot$ produces a considerable outflow with a realistic wind velocity even though no dust is present to drive the wind (see Fig. 9). In this context it is interesting to note that for the O-rich wind models the outflow velocity does not depend on $\Delta u_{\rm p}$ while the mass loss rate increases with this parameter, demonstrating its influence on the density (levitation, see Sect. 3.2). The combined results for velocity and mass loss therefore indicate that the driving force (i.e. radiation pressure on molecules) in these O-rich models is relatively insensitive to the density, in contrast to the formation of dust which provides the necessary opacity for the radiation-driven winds in our C-rich models.

In general, the phenomenon of an outflow (partially) driven by radiation pressure on molecules as seen in our present models is a likely scenario for luminous cool stars. But no strict quantitative conclusions should be drawn from the models presented here since they are based on grey radiative transfer which is a crude assumption for evaluating the radiative pressure term. However, the tendency of Planck means to over-estimate radiative pressure on molecules might be compensated by the fact that the effect of Doppler shifts on the flux-integrated absorption coefficient is neglected in grey dynamical models.

Note also, that the driving by molecules only becomes efficient in the dynamical models where the radiation pressure acts on material which has already been lifted to cooler layers by the pulsation-induced shocks waves. All of the non-pulsating

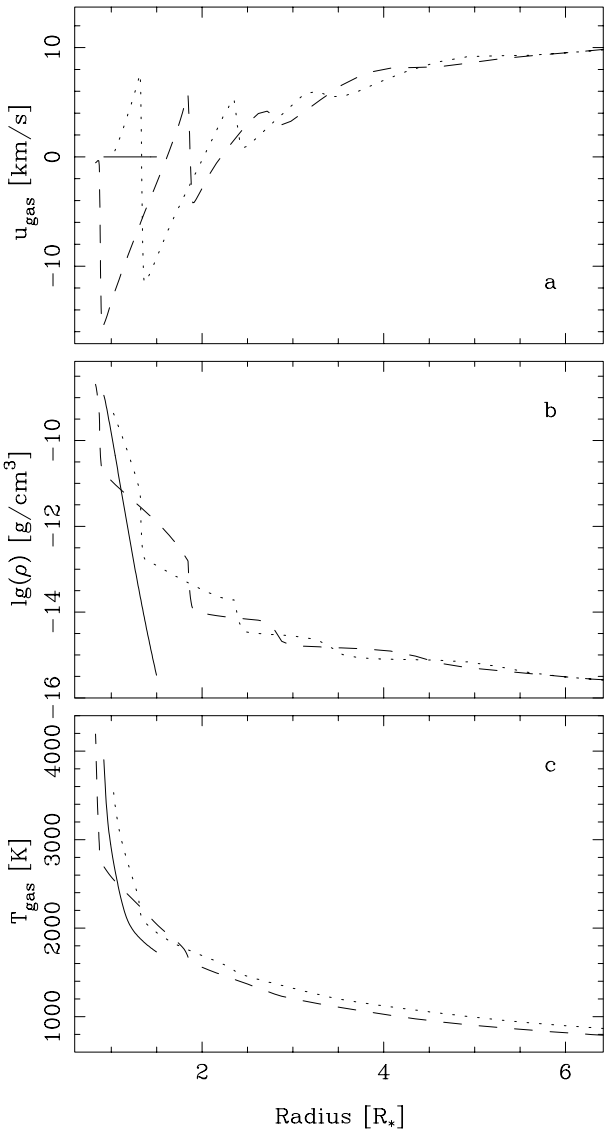

Fig. 9a–c. Radial structure of model P7OU4 at different phases (0.50: dashed, minimum light; 1.00: dotted, maximum light) and of the corresponding hydrostatic initial model (full line); flow velocity **a**, gas density **b** and gas temperature **c** as a function of the radius (given in units of the radius of the hydrostatic initial model). The wind of this O-rich model is driven by radiation pressure on molecules (no dust formation included).

(dust-free) initial models are strictly hydrostatic, i.e. show no tendency to form a radiation-driven outflow.

5. Conclusions

In recent years the dramatic quantitative and qualitative increase of observational data on AGB stars has demonstrated the shortcomings of standard hydrostatic model atmospheres. On the other hand, considerable progress has been achieved in dynamic models of the circumstellar envelope and stellar winds.

A relatively crude approximation that is imposed on state-of-the-art dynamic model atmospheres by computing time requirements is the restriction to grey radiative transfer. Nevertheless, such models are the only self-consistent method to investigate the effects of various time-dependent dynamical phenomena (shocks, winds) on observable properties of pulsating AGB stars. When based on reasonable mean opacities present dynamic model atmospheres can give us at least a qualitative understanding of physical processes in long-period variables.

The hydrostatic limit case provides an opportunity to test the effects of grey radiative transfer (and other approximations) by comparing the atmospheric structures to classical model atmospheres which include a detailed frequency-dependent treatment of the radiative transfer. We find that using Planck mean absorption coefficients based on detailed molecular line data yields atmospheric structures which are in much better agreement with standard model atmospheres (based on the corresponding frequency-dependent opacities) than models using a constant value of the absorption coefficient (as often done in similar models in the literature). The large deviations in the uppermost layers of the hydrostatic Planck mean models from the corresponding opacity sampling models are most likely due to the grey treatment of radiative transfer but the relevance of this differences is probably limited as these atmospheric layers are dramatically influenced by dynamical processes. However, we can conclude here that the inner part of the initial and the hydrodynamical models is obviously considerably improved in going from a constant gas absorption coefficient as used in many earlier dynamic models to a realistic, density- and temperature-dependent Planck mean absorption coefficient.

The propagating shock waves caused by stellar pulsation modify the atmospheric background structure in a way which cannot be simulated with a sequence of standard hydrostatic model atmospheres. The effects of time-dependent dynamics on the structure are of the same order of magnitude as the errors due to grey radiative transfer. This seems to be a likely explanation why hydrostatic models fail to reproduce certain observational facts, no matter how sophisticated their physical input data and radiative transfer actually are. On the other hand, experimental calculations seem to indicate that our dynamic models are able to reproduce observed molecular features and out-of-phase variations in the spectra of long-period variables.

The gas opacity used in the dynamic models considerably influences the stellar wind properties, due to its strong effect on the atmospheric structure. A change in the gas density at a given temperature affects both, the efficiency of the dust formation and the mass loss rate. Moreover, the influence of the carbon-to-oxygen ratio on the gas opacity (which was neglected in previous C-rich time-dependent models) could lead to a qualitatively different dependence of the wind properties on this parameter in C-stars. Since the same molecules that are involved in the formation of carbon grains contribute significantly to the opacity, a certain self-regulating mechanism exists for the chemical abundances and the gas density. Therefore, the simple rule that an increased carbon overabundance leads to more efficient dust formation may not be valid when molecular opacities are taken into account. Furthermore, our dynamical models indicate that radiation pressure on molecules may contribute to driving stellar winds of both O- and C-rich stars. However, due to the fact that the models are based on Planck mean gas opacities no detailed quantitative conclusions should be drawn yet.

The present dynamic model atmospheres are a first step in trying to understand the influence of time-dependent dynamics on observable quantities of AGB stars. The construction of more sophisticated models which, e.g., combine detailed frequency-dependent radiative transfer and dynamic processes in a self-consistent way is an important future goal. Furthermore, the simple piston boundary condition presently simulating stellar pulsation should be replaced by variations derived from pulsation models. The long-term perspective is a simultaneous computation of both the pulsation zone and the atmosphere and stellar wind region. However, if the dynamic model atmospheres may not yet be enough advanced for a detailed quantitative interpretation of observational results they give at least a self-consistent qualitative picture which can help us to understand intrinsically time-dependent phenomena such as the effects of pulsation.

Acknowledgements. This work is supported by the Austrian Science Fund (FWF, grants J01283-AST, J1487-PHY and S7308-AST). We thank M. Feuchtinger (IfA Vienna) for his help with the grey initial models, B. Plez (Lund, Uppsala) for providing chemical data, and both of them, as well as E.A. Dorfi, J. Hron and G. Wuchterl (IfA Vienna) for inspiring discussions.

References

Alvarez R., Plez B., 1998, A&A 330, 1109
Aringer B., Jørgensen U.G., Langhoff S.R., 1997a, A&A 323, 202
Aringer B., Kerschbaum F., Jørgensen U.G., et al., 1997b, In: Proc. First ISO Workshop on Analytical Spectroscopy. ESA SP-419, p. 249
Aringer B., Höfner S., Wiedemann G., et al., 1998, A&A, submitted
Arndt T.U., Fleischer A.J., Sedlmayr E., 1997, A&A 327, 614
Beach T.E., Willson L.A., Bowen G.H., 1988, ApJ 329, 241
Bessell M.S., Scholz M., 1989, In: Johnson H.R., Zuckermann B. (eds.) IAU Coll. 106, Evolution of Peculiar Red Giant Stars. Cambridge Univ. Press, p. 67
Bessell M.S., Brett J.M., Scholz M., Wood P.R., 1989, A&A 213, 209
Bessell M.S., Scholz M., Wood P.R., 1996, A&A 307, 481
Bowen G.H., 1988, ApJ 329, 299
Fleischer A.J., Gauger A., Sedlmayr E., 1992, A&A 266, 321
Gustafsson B., Bell R.A., Eriksson K., Nordlund Å., 1975, A&A 42, 407
Gustafsson B., Jørgensen U.G., 1994, A&AR 6, 19
Helling C., Jørgensen U.G., 1998, A&A 337, 477

Höfner S., Dorfi E.A., 1997, A&A 319, 648 (HD97)
Höfner S., Feuchtinger M., Dorfi E.A., 1995, A&A 297, 815
Höfner S., Jørgensen U.G., Loidl R., 1998, Ap&SS 255, 281
Hron J., Aringer B., Loidl R., et al., 1997, In: Proc. First ISO Workshop on Analytical Spectroscopy. ESA SP-419, p. 213
Hron J., Loidl R., Höfner S., et al., 1998, A&A 335, L69
Jørgensen U.G., 1997, In: van Dishoeck E.F. (ed.) Molecules in Astrophysics: Probes and Processes. Proc. IAU Symp. 178, Kluwer, p. 441
Jørgensen U.G., Johnson H.R., Nordlund Å., 1992, A&A 261, 263
Loidl R., Hron J., Höfner S., et al., 1997, Ap&SS 251, 243
Loidl R., Hron J., Aringer B., Höfner S., Jørgensen U.G., 1998, Ap&SS 255, 289
Tsuji T., Ohnaka K., Aoki W., Yamamura I., 1997, A&A 320, L1
Willson L.A., Bowen G.H., 1998, In: Kaper L., Fullerton A.W. (eds.) Cyclical Variability in Stellar Winds. ESO Astrophysics Symposia, Springer, p. 294
Windsteig W., Dorfi E.A., Höfner S., Hron J., Kerschbaum F., 1997, A&A 324, 617
Windsteig W., Höfner S., Aringer B., Dorfi E.A., 1998, In: Kaper L., Fullerton A.W. (eds.) Cyclical Variability in Stellar Winds. ESO Astrophysics Symposia, Springer, p. 308
Winters J.M., Fleischer A.J., Le Bertre T., Sedlmayr E., 1997, A&A 326, 305
Woitke P., Krüger D., Sedlmayr E., 1996, A&A 311, 927
Wood P.R., 1990, In: Mennessier M.O., Omont A. (eds.) From Miras to Planetary Nebulae: Which Path for Stellar Evolution? Editions Frontieres, Gif sur Yvette, p. 67